Authors' accepted manuscript of the article to be published in
IEEE Transactions on Smart Grid
http://dx.doi.org/10.1109/TSG.2016.2548944

An Impedance Based Method For Distribution System Monitoring

Hashem Mortazavi, *Student Member, IEEE*, Hasan Mehrjerdi, *Member, IEEE*, Maarouf Saad, *Senior Member, IEEE*, Serge Lefebvre, Dalal Asber and Laurent Lenoir

***Abstract*—This paper presents a new approach in monitoring of a power distribution system. It uses the bus voltage and injected current to extract the apparent impedance seen from the measuring unit location. Then the apparent impedance variation is used for monitoring of different electrical quantities of the feeder such as feeder power factor, the minimum and maximum of active and reactive power flow. The paper also presents the mathematics for defining monitoring zone on the *R-X* plane to detect those parameters variations. The proposed method was tested with the unbalanced distribution system feeder loading, distributed and lumped model of solar and wind power generations. OpenDSS and Matlab are used to test the effectiveness of the method with the IEEE 8500 node test feeder. The dynamic performance of the proposed method is studied for on-line monitoring of the reactive power capability requirement of a Canadian utility for a wind farm integrated to the system. The results show that the monitoring method based on the apparent impedance has a good capability to detect different operation conditions. In addition, the simplicity of the proposed method allows easy application of it in smart grid and traditional distribution system.**

***Index Terms*— Smart grid, renewable energy resources, monitoring, impedance measurement, reactive power capability.**

I. Introduction

Based on the equipment failures data and statistics, electric distribution systems, due to high number of feeders have the highest rate of customer supply unavailability (supply interruption) in power systems [1]. Network automation, newer protection philosophy, deployment of monitoring technique, coordinated Volt-VAR control, fast fault detection technique, improving the feeder load balancing and voltage regulation are the main technique to improve the customer service quality and distribution system reliability.

Widespread real-time monitoring of distribution system, because of the high number of feeders and lack of the communication system was impossible for a long time. By decreasing the price of communication system, full deployment of smart meters seems applicable for implementing the smart grid in distribution system level. Monitoring of distribution system due to its time varying and unbalanced loading, through smart meters and monitors is one of the basis of smart grid [2]. Different monitoring system approaches and devices have been proposed to assess different conditions of distribution systems. Power quality monitoring system has been used for a long time not only for analyzing power quality issues but also for load modeling [3]. Qiang et al in [4] proposed a voltage monitoring for micro grid application, to analyze the power quality and reliability indexes. Using state estimation technique is one of the most popular solutions proposed in the literature for distribution system monitoring. The authors in [5] propose using the on-line system modelling capability of artificial neural network (ANN) for distribution system state estimation. The application of branch current state estimation method has been proposed in [6],[7] for real time monitoring and control of a distribution feeder. Authors in [8] proposed an ANN based monitoring system for better voltage magnitudes estimation of distribution feeder in presence of distributed generation (DG). Powalko et al. in [9], proposed to use phasor measurement units (PMU) for improved distribution system state estimation.

The renewable energy sources (RES) network integration affects the traditional Volt-VAR control, power factor correction and voltage regulation [10-12]. High PV penetration impacts on distribution system protection and operation were analyzed in [13]. Unidirectional power flow was the first design criteria for distribution system planning for decades. Under this assumption the voltage profile is maximum at the feeder head and decreases proportional with loads to the end of the feeder [14]. Depending on the size and location of variable generation and the load size the power flows may reverse in the feeder [2].Therefore, the current distributions system vulnerability increases by RES generation. The high RES penetration increases the necessity of deployment of monitoring devices for different purposes.

Mortazavi et al proposed an impedance based monitoring technique for reverse power flow detection in [15]. It was shown that the apparent impedance is sensitive to small load variation. Its changes correspond to distributed generation variations and it has a very good capability for reverse power flow detection on each phase, separately. In addition, the dynamic application of impedance monitoring technique was validated for fast transient conditions such as cloud movement impacts on solar farm. Based on the interconnection standard, by RES integration to distribution system, utilities need to install distance relay as the main feeder protection device. In [16], authors propose using the distance relay not only as a

This work was supported by the Research Institute of Hydro-Quebec(IREQ), Power Systems and Mathematics, Varennes, QC, Canada

H. Mortazavi, and M. Saad are with the Department of Electrical and Computer Engineering, Quebec University (ETS), Montréal, QC, Canada(e-mail: hashem.mortazavi.1@ens.etsmtl.ca).

H. Mehrjerdi is with Qatar University, Doha, Qatar.

S. Lefebvre, D. Asber and L.Lenoir are with the Research Institute of Hydro-Quebec (IREQ), Power Systems and Mathematics, Varennes, QC, Canada.

protection device, but also as a monitoring tool at presence of renewable energies.

There are very few publications regarding monitoring of MV and LV feeders in distribution systems despite many smart meter applications for the residential and commercial consumers. It was shown that by RES integration to distribution system the distribution system changes from a passive network to an active network with dynamic characteristics [10]. This paper proposes the idea of an integrated feeder power flow monitoring technique based on impedance measurement. The paper presents, the mathematics needed for mapping monitoring zone from *P-Q* plane onto the *R-X* plane. It used to detect power factor variations and active and reactive power flows beyond the pre-defined limits. In addition, it will be shown that based on the proposed transformation, any complex monitoring zone in the *P-Q* plane can be transferred to the *R-X* plane. The dynamic performance of the proposed method is studied with the unbalanced IEEE 8500 node test feeder, for on-line monitoring of the reactive power capability requirement proposed by the Alberta Electric System Operator (AESO) [17] for a wind farm integrated to the system.The paper is organized as follows: in Section II the necessity of distribution system monitoring will be explained. Section III describes the mathematic relationship between the active and reactive power flows and the measured impedance trajectories. Section IV presents the IEEE 8500 node test feeder as case study and the simulation results will be presented in Section V. Finally the conclusion is presented in Section VI.

II. Distribution System Monitoring Necessity

As it was stated in introduction, contrary to transmission systems, due to high number of feeders and elements, distribution systems suffers lack of sufficient monitoring devices. In this section some challenges which raise the necessity of deployment of monitoring units in distribution network will be presented briefly.

- Distribution systems have been designed for radial and unidirectional power flow. In this design the active and reactive power are transferred from the transmission system to consumers. Therefore, many protection and voltage regulation strategies in distribution networks are based on this radial nature. For example, voltage regulators are designed with the flow of power from the higher voltage to the lower voltage. Integration of the RES to distribution systems, however, shows that based on the size and the installation location, the power flow may reverse [18]. For high penetration of RES, traditional unidirectional distribution system will change to a bidirectional system which needs a revision of regulation.
- The minimum voltage drop which must be kept within standard limits was the main concern of distribution system planner for a long time. On the other hand, the feeder overvoltage was not a concern for distribution system design. With RES integration the over-voltage possibilities become one of the main design concerns [10].
- From a practical standpoint the real distribution system has non-uniform load distribution, distributed load location and different wire size. The designer considers increased wire size for contingency-support branches during special situations [19]. Distributed RES integration with intermittent characteristic, increases the vulnerability of small wire size feeder to overload conditions.
- In addition, in a unidirectional power flow design philosophy, the designer consider feeder load balancing, through opening and closing switches at different locations, as an economical solution regarding the load growth over the time. Due to changing the switch patterns, the distribution network configuration is a dynamic variable [20]. The RES generation will increase this dynamic characteristic which justifies the capital cost needed to deploy new monitoring techniques.
- Moreover, Volt-VAR control, power factor correction and voltage regulation are important elements for increasing the distribution system efficiency in operation. Reactive power flow on a feeder decreases its active power flow capacity and increases both the voltage drop and loss. In a unidirectional distribution network, even feeders with in-range power factor correction at the substation have portions that are not corrected well (particularly at the feeder's end, where the power factor is much lower) [19]. The capacitor size needed to correct power factor during peak VAR conditions (during summer due to the high reactive loads of air conditioning system) may seriously over-compensate during off-peak conditions. A survey made by H. L. Willis [20] indicated that slightly more than one-third of all switched capacitor banks were not switching properly due to mechanical failure, vandalism, or weather conditions.

In this section, it was argued that the modern distributions system vulnerability increases not only because of infrastructure aging, but also, because of RES generation. It increases the necessity of deployment of monitoring devices for different purposes. In the next section it will be shown that the apparent impedance measured on the feeder has great capabilities for on-line monitoring of distribution feeders.

III. Measured Impedance Trajectory and Power Flow

In the last section, it was mentioned that there are different situations in distribution systems which need more attention in order to improve network operation. The capability of the impedance based method for reverse power flow detection was shown in [15]. In this paper it will be shown that the apparent impedance has a good potential for monitoring of feeder power factor, in addition to reverse and forward active and reactive power flow.

A. Impedance measurement

The apparent impedance seen from any point on a feeder is calculated by three single phase measuring units. Each unit uses only a single phase current and a single phase voltage. Considering that V_{AN} is the phase *A* to ground voltage and I_A is the current flows through the phase *A* conductor, the apparent impedance seen for phase *A* is given by [21]:

$$Z_A = \frac{V_{AN}}{I_A} \quad (1)$$

The impedance calculated using (1) is the positive sequence impedance for all system operation condition except fault conditions [21]. In practical application, the feeder grounding must be checked and in order of accurate V_{AN} and I_A measurement, maybe grounding transformers are needed to be installed [22].

B. Mapping between P-Q and Z plane

The mapping concept will be used to develop the relationship between the measured impedance and power flow quantities. To do so, for an impedance measuring unit , located at sending end of Fig.1 (bus 1) the apparent impedance measured by an impedance measuring unit is calculated by [15]:

$$|\bar{Z}| = \frac{|\bar{V}|}{|\bar{I}|} = \left(\frac{P + jQ}{P^2 + Q^2}\right) \times |V|^2 = \frac{|V|^2 \times \bar{S}}{|\bar{S}|^2} \quad (2)$$

Where, $\bar{Z}$ is the apparent impedance obtained by measuring unit installed at *bus 1*, $\bar{I}$ is the line current flow from *bus 1* to *bus 2*, measured by a phase CT (current transformer), $\bar{V}$ is the measured line to ground voltage of *bus 1* by a one phase VT (voltage transformer), $\bar{S}$ is the apparent power, and P, Q are the active and reactive powers transmitted from *bus 1* to *bus 2*, respectively.

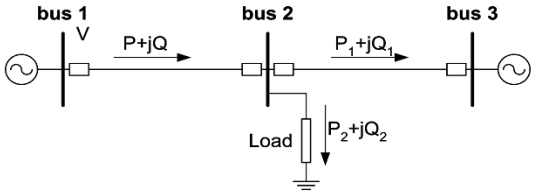

Fig.1. Simple two source system power flow [23].

Eq. (2) shows the relationships between the measured apparent impedance at bus 1 and the active and reactive power transmitted through the line, and it can be used for mapping between the *P-Q* plane and *R-X* plane. The measured $\bar{Z}$ is a complex value and has real and the imaginary part which are written as [15]:

$$R = \left(\frac{|\bar{V}|^2}{P^2 + Q^2}\right) \times P \quad (3)$$

$$X = \left(\frac{|\bar{V}|^2}{P^2 + Q^2}\right) \times Q \quad (4)$$

The sum of squared of (3) and (4) are written as:

$$R^2 + X^2 = \frac{|\bar{V}|^4}{P^2 + Q^2} \quad (5)$$

For fixed apparent power, Eq. (5) is a circle with fixed radius: $\frac{|\bar{V}|^2}{\sqrt{P^2+Q^2}}$ and center coordinates of $(0,0)$. The measured impedance loci for fixed apparent power condition are shown in Fig.2. The load power factor variations determine the impedance loci direction in *R-X* plane. For variable load power factor, the 'd_1' direction in circle 'C_1' shows the impedance loci while the load power factor decreases (or the load power factor angle φ increases). For fixed load power factor, the impedance locus is illustrated by line 'a' in Fig.2.

The 'd_2' direction in line 'a' shows the impedance loci for fixed load power factor, while the transmitted apparent impedance increases. For variable power factor the apparent impedance loci moves in a circle loci. The circle 'C_1' shows the impedance loci for this condition. The radius of the circles is inversely proportional to apparent power magnitude. By increasing apparent power magnitude the circle radius decreases and vice versa. Therefore, the circle "C_2" represents the heavier load condition in comparison with the circle "C_1".

Moreover, Eqs. (3) and (4) show that the location of calculated apparent impedance in R-X plane depends on the value and direction of transmitted active and reactive power from bus 1 to bus 2. The sign of *R* in (3) and *X* in (4) are only related to the sign (direction) of *P* and *Q*, respectively. Table. I explains the relationship of R and X sign of calculated impedance with the actual active and reactive power flow direction [24]. As each point R-X corresponds one-to-one to a point in P-Q plane, therefore, the R-X plane has the capability to react to every change in the P-Q plane.

Table I. Explanation of R and X sign

Condition	Sign of R	Sign of X
Power Flow from Bus *1* to *2*	Positive	
Power Flow from Bus *2* to *1*	Negative	
Lagging Reactive Power from Bus *1* to 2		Positive
Lagging Reactive Power from Bus 2 to *1*		Negative
Leading Reactive Power from Bus *1* to 2		Negative
Leading Reactive Power from Bus *2* to *1*		Positive

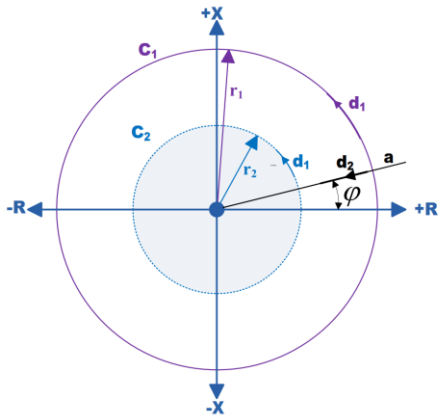

Fig.2. Measured impedance trajectories for active and reactive power variation while the apparent power is fixed.

C. Special Cases

In the last section the general equation for mapping the *P-Q* plane to *R-X* plane was derived. There are several special considerations in distribution system design and operation. In this section basic mathematic will be presented for special cases such as conversion of fixed active or reactive power limit to the *R-X* plane. Later these special cases will be used to analyze more complex situations.

Considering the Fig.1, $\bar{V}$ is the measured line to ground voltage at bus 1, and P, Q are the active and reactive powers transmitted from bus 1 to bus 2, respectively. Eq. (6) is used for calculating the voltage drop along the feeder [10].

$$\Delta V = \frac{[R \times P + X \times Q]}{V^2} \quad (6)$$

Eq. (6) indicates that the voltage drop is related to line power flows. In distribution system design each feeder has a

predefined voltage drop for minimum and maximum feeder load which must be in standard region. With RES integration the voltage drop varies depending on the RES generation, its location and feeder consumption. The compensated voltage drop is the main cause of feeder over voltage. Reference [10] showed that the negative voltage drop not only occurs at reversed power flow but may also happen at low forward power flow. Utilities use low forward power relays in order to control (or prevent) power flow on some special lines in the network [25].

1) Minimum forward reactive power flow limitation

In distribution system design the minimum and maximum reactive power transferred through the feeder are used for capacitor banks size selection and their optimal location [20]. As it is shown in Fig.3 Q_0 is considered as the minimum designed reactive power flow on the line. To find the mapping of the hatched region for $Q>Q_0$, where $Q_0>0$, in *R-X* plane, first the line will be mapped on the R-X plane then the mapping of $Q>Q_0$ region will be found.

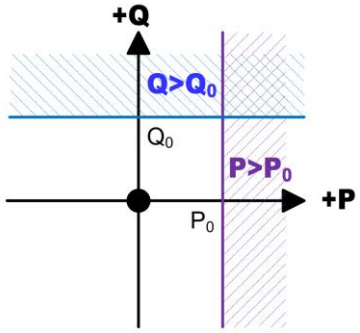

Fig.3. Defined minimum active and reactive power regions on the P-Q plane.

Note that the straight line Q_0 in Fig.3 has a finite length. By substituting (4) into (5) results in:

$$R^2 + X^2 = X \times \frac{|\bar{V}|^2}{Q_0} \qquad (7)$$

Eq. (7) can be re-arranged as:

$$R^2 + (X - \frac{|\bar{V}|^2}{2Q_0})^2 = \frac{|\bar{V}|^4}{4Q_0^2} \qquad (8)$$

For fixed reactive power, Eq. (8) is a circle with radius: $\frac{|\bar{V}|^2}{2Q_0}$ and center coordinates of $\left(0, \frac{|\bar{V}|^2}{2Q_0}\right)$. As the line Q_0 is not infinite the final mapping is an arc instead of a complete circle (missing the original of *R-X* plane).

This circle is illustrated in Fig.4 as curve 'C_1' and traces the trajectory of the measured impedance, which moves in the ' d_1' direction as the real power increases. For $Q>Q_0$, the (8) is written as:

$$R^2 + (X - \frac{|\bar{V}|^2}{2Q_0})^2 \leq \frac{|\bar{V}|^4}{4{Q_0}^2} \qquad (9)$$

Eq. (9) shows the final region as all the points inside the circle 'C_1'. In the same manner, the transforming region of $Q<Q_0$ is all the points outside of circle 'C_1'.

2) Minimum active power flow limitation

Consider P_0 as the minimum designed active power flow on the line. To find the mapping of hatched region for $P>P_0$ where $P_0>0$ in *R-X* plane, substituting (3) into (5) results in:

$$R^2 + X^2 = R \times \frac{|\bar{V}|^2}{P_0} \qquad (10)$$

This can be re-arranged as follows:

$$(R - \frac{|\bar{V}|^2}{2P_0})^2 + X^2 = \frac{|\bar{V}|^4}{4{P_0}^2} \qquad (11)$$

For fixed active power, Eq. (11) is a circle with radius: $\frac{|\bar{V}|^2}{2P_0}$ and center coordinates of $\left(\frac{|\bar{V}|^2}{2P_0}, 0\right)$. In Fig.4 this circle is illustrated as 'C_2'. Based on (11) when the transmitted reactive power increases the impedance locus moves in 'd_2' direction. The region of the R-X plane corresponding to (11) and for $P > P_0$ is the region inside the circle 'C_2'.

3) Fixed power factor

Distribution system operator usually prefers unit power factor or close to unity, because of the corresponding reduction of the line losses due to less reactive power flow. The tendency to increase the level of penetration of renewable energy sources, and the effect of those variable sources on the feeder power flow and voltage regulation urges the utilities to put some limitation at the point of interconnection (*POI*). For example FERC predetermined the reactive capability requirement up to 0.95 lag to lead at the POI for wind power generation in FERC Order 661-A [26].

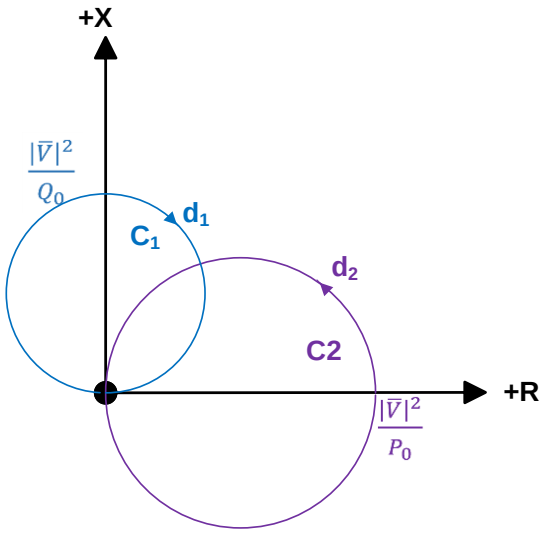

Fig.4. Measured impedance trajectories for active and reactive power variation.

Fixed power factor operation of feeder is a line in *P-Q* plane. For mapping that from *P-Q* plane to *R-X* plane, (4) divided by (3) results in:

$$\frac{X}{R} = \frac{Q}{P} = \tan\varphi \qquad (12)$$

Where φ is defined as the feeder power factor angle. Eq. (12) shows that mapping a straight line passing through the origin in *P-Q* plane is a straight line passes through the origin in *R-X* plane.

IV. Case Study

To show the capability of impedance based monitoring technique, the IEEE 8500 Node Test Feeder (Fig.5) is chosen.

As presented in [27], the 8500 node test feeder is a relatively large network that has 2516 medium voltage nodes, all type of line configurations such as single, two and three-phase MV and LV lines. It has four voltage regulators, one installed at substation and three distributed along the feeder. The circuit also contains three controlled and one uncontrolled capacitors banks. The settings of the voltage control devices were set at their nominal values in the simulations. When the reactive power flow in the line is 50% of the capacitor size, the capacitor controller switches it ON and when the flow is 75% of the capacitor size in the reverse direction switches it OFF.

As this model is a large, heavy loaded, consisting of three-phase and one-phase overhead lines and cables, it is a good case for testing the impedance method monitoring capabilities.The GridPV toolbox[28] is used as a COM server interfaced between OpenDSS [29] and the Matlab [30] for system simulation.

For RES simulation, there are different choices such as solar PV, wind turbine, biomass and small hydro turbines. In this research, both the PV system and wind turbine model provided in OpenDSS are used as the RES model. Both the lumped and distributed model of PV system are installed at different locations to analyze the generation location impact on the measured apparent impedance.

Hoke et al. in [31] showed that the 15-20% limit for PL studies is very conservative for most of feeders in distribution network. They showed that in more than 66% of the simulated cases, the maximum PL is greater than 90%. Therefore for simulation of different penetration level (PL) impact analysis, the PV generation was increased from zero to 1.15 pu of the nominal size of PV unit. At each step, the PV output increased one percent and then a power flow was run with OpenDSS. Power flow solutions (voltages, currents, active and reactive power of feeder) were sent to MATLAB through the COM server interface. Then those data were analyzed by GridPV toolbox and user written scripts. The simulation results are shown for unit power factor operation of PV systems, otherwise it will be mentioned.

V. Simulation Result and Discussion

A. Reverse power flow detection

Based on Eq. (2) the measured impedance can be used as a tool for reverse power flow detection. For a radial distribution system design, the reverse power flow causes over voltages in some part of a feeder. According to the Eqs (3) and (4) the measured R and X signs have a direct relationship with active and reactive power signs, respectively. To simulate the reverse power flow, 14 distributed PV units with different sizes in range of 100, 200 and 300 kW with total generation of 3700 kW are installed at different locations based on the nominal load of the line.

Fig.6 shows the exact value of active and reactive power for each feeder according to the distance from the substation. As it can be seen, the reverse active power happens at some locations (only on phase-A and phase-C around 7 km from the substation). Regarding reactive power flow, Fig. 6 shows numerous reverse reactive power at different locations due to presence of switched and unswitched capacitor bank distributed along the feeder.

Fig.7 shows the apparent impedance loci measured at three different measuring units' location. The measuring unit locations are chosen according the [27]. The apparent impedance measuring units' location are shown in Fig. 5.

Fig.7-a shows the measured impedance in each phase at measuring point M1 (installed at bus L2955077). Sudden changes in the measured impedance loci are related to substation and feeder voltage regulator tap changer variation.

While Fig.7-a shows the forward active and reactive power flow on the line LN6381853-1, Fig.7-b shows the reversed reactive power flow with forward active power flow on the line LN6109158-1 due to a 900 kVAr capacitor bank installed downstream the measuring point M2 (bus:L2936279).

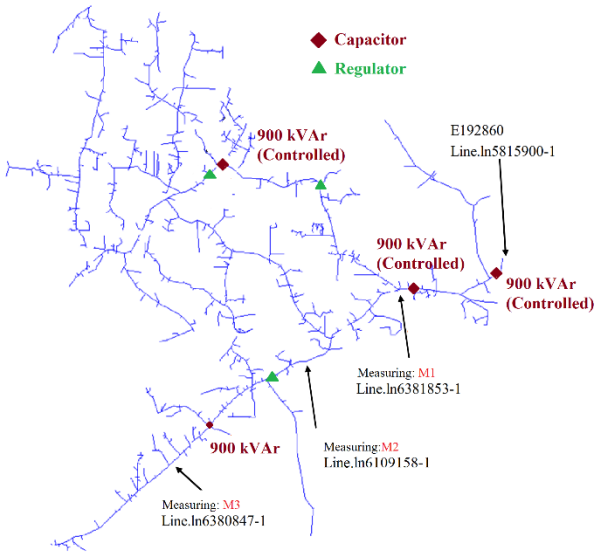

Fig 5. Schematic of The IEEE 8500 Node Test Feeder [27].

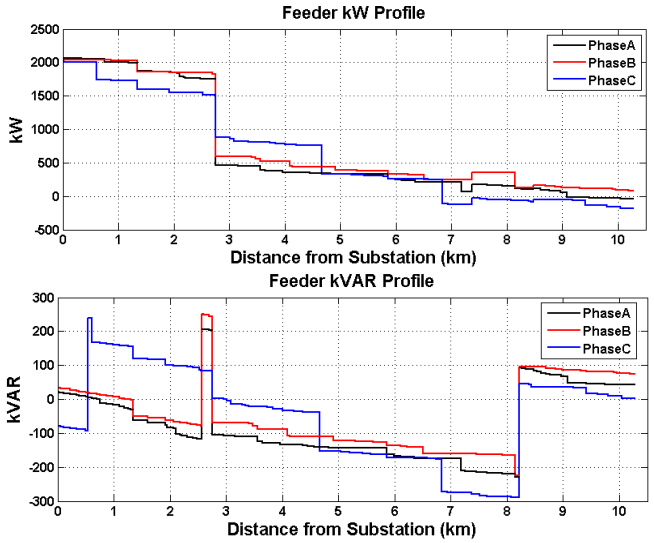

Fig. 6. All feeder active and reactive power based on the distance from substation.

For measuring unit M3, unlike the phase-B in Fig. 7-c the phases A and C show the reversed power happens at different PL. For the phase A, at PL=108% the R becomes zero and after this point the R goes negative corresponding the reversed

active power. The reason for the decreasing R is related to the relationship between the measured R and total P and Q flows along the line. Based on equation (3) by decreasing the P -due to the increased PV penetration level - the measured R will decrease too. While the impedance location for the phase A is entered to the second quarter of R-X plane (for PL=108%) showing small reversed active power, the phase C shows a higher reversed active power started at PL=73%. This phenomenon happens due to the unbalanced operation of IEEE 8500 node test feeder. Based on the Eq.s (3) and (4), the apparent impedance measured at any location, has a direct relationship with RES penetration level and reverse relationship with transferred power. The larger the power transferred through the line (equal to low RES penetration level), the smaller measured R and X and vice versa.

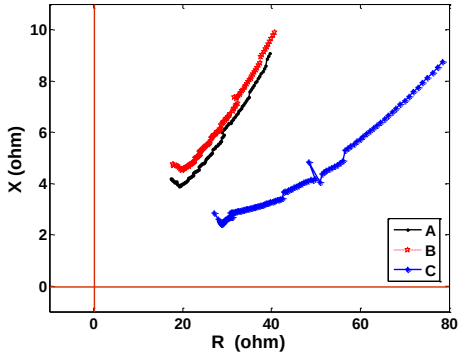

a- Measured impedance at measuring point M1- three phases.

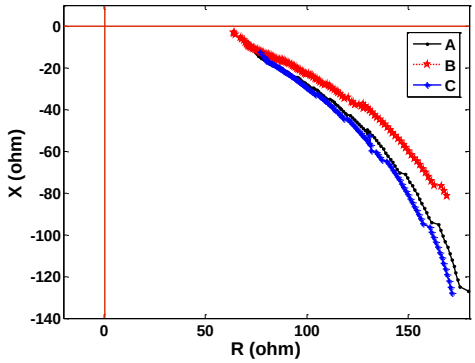

b- Measured impedance at measuring point M2- three phases.

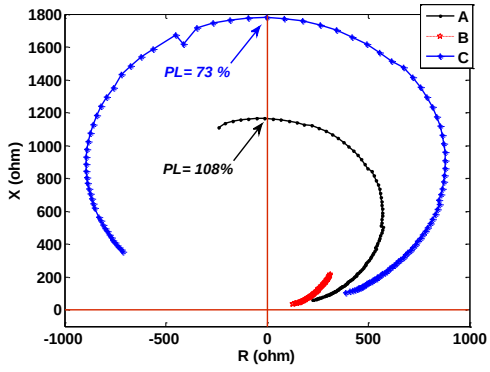

c- Measured impedance at measuring point M3- three phases.

Fig. 7. Measured impedance at Bus 632 for lumped PV installed at bus 680.

Unbalance operation is an intrinsic characteristic of distribution system. This unbalance operation has different causes such as, feeder unbalanced load, time varying and nonlinear loads and feeders configuration. Therefore, it is anticipated that when the voltage and current of the three phases are unbalanced the resultant calculated impedance for each phase is not the same as other two phases. This unbalanced operation of distribution system was shown in the Fig. 7. The three phase calculated impedances at those metering locations, not only have not the same values, but also shows different patterns for PL variations. For example, unlike the phase B as shown in Fig.7-c, the phase A and C undergo reverse power active power at different PLs. Therefore, due to unbalance operation of distribution system, any proposed monitoring technique shall have the capability for separate three phases monitoring.

Fig. 8 shows the IEEE 8500 node test feeder power flow direction produced by GridPv toolbox at a snapshot of system (at the PL=100%). While the number of monitoring points are limited in a real distribution system, Figs 7 and 8 show that the reversed power happens not only at different locations, but also may be happens at one or two phases only.

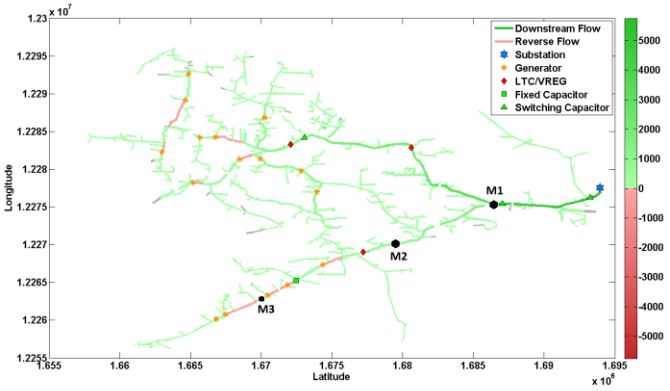

Fig.8. IEEE 8500 node test feeder power flow direction for PL=100%. The red colors shows the reversed power flow part of feeder. The PV units' location are shown by Orange stars.

B. Monitoring the feeder PF

In general, maintaining the feeder power factor as close as possible to unity is a goal in distribution system design as long as the voltage level lies within the allowable range. However, maintaining a unity power factor could result in high number of operations of voltage regulating equipment which will decrease the equipment maintenance period and make it uneconomical. Therefore a range of power factor variation is always defined. For example, based on the Hydro-Quebec interconnection guideline, the customer load at the connection point must have a power factor of 95% or higher for large-power customers and 90% or higher for medium- and small-power customers.

Fig.9-a shows a snapshot of the IEEE 8500 feeder power factor for the maximum PV penetration level, for the same condition of the last section (14 distributed PV units). Fig. 9-b is a part of Fig. 9-a zoomed in, and this snapshot clearly shows that some feeders suffer from low power factor. This mostly happens near the RES point of connections. According to the Eqs (12), the simple explanation of this phenomenon is the

variation of ratio of active power to apparent power, transmitted through feeder, due to the PV generation. In this simulation all the 14 PV units operates at unity power factor.

For acknowledgment by the distribution system operator, a set of feeder over-excitation and under-excitation alarms were defined for each monitor based on the Eq. (12). The set points are defined for pf =±0.90 for each monitor. For values detected beyond those limits, an alarm will be issued. Fig. 10 shows the output of alarm system for PV penetration level variation. It can be clearly seen that only monitor M3 detects over excitation condition only on the phase-A (alarm starts at PL= 82%) and the phase-C (alarm starts at PL= 56%). The comparison of Figs. 7 and Fig.10 shows that although the measuring point M2 shows the continuous under-excited condition (reversed reactive power only) for all the phases of that feeder, at any conditions the feeder power factor goes beyond the pre-defined settings (maintain its power factor between 0.90 and unity).

Comparison of Fig.8 and Fig.9 emphasizes the necessity of installation of the monitoring units for critical feeder and points of high RES integration, because the feeder electric parameters may go beyond the distribution system designer limits.

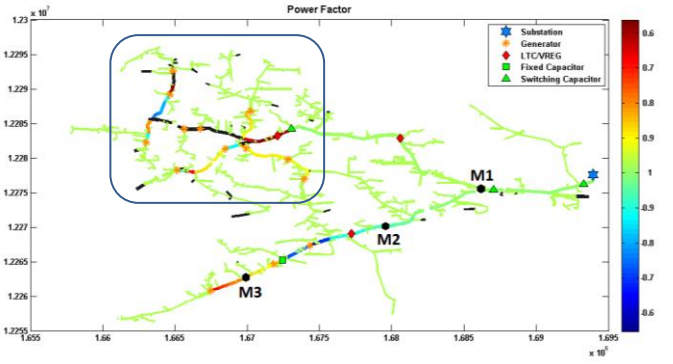

a- IEEE 8500 node test feeder.

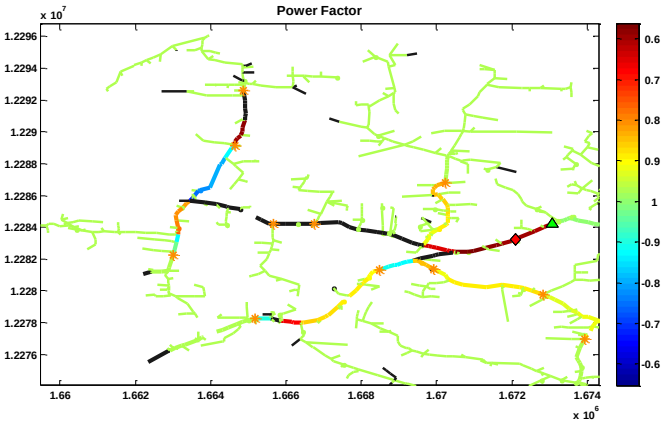

b- The zoomed in part of the IEEE 8500 node test feeder.

Fig.9. IEEE 8500 node test feeder power factor variation. The blue spectrum feeder shows the lagging (capacitive) pf>1 and the red spectrum shows the leading (inductive) pf<1. The PV units' location are shown by Orange stars.

C. Practical implementation of monitoring method

In order of reliable operation of power system, the generating units must comply with certain reactive power requirement depending on the network they are connected. Although many of existing interconnection regulations have been based on traditional generating units' capabilities, the increasing rate of RES integration forces the power system regulators to consider variable type of generation in their standards and practical procedures. IEEE 1547 standards, as a base regulation for RES integration in North America, banned operating in voltage or reactive power control mode for distribution level connection of PV and wind turbine.

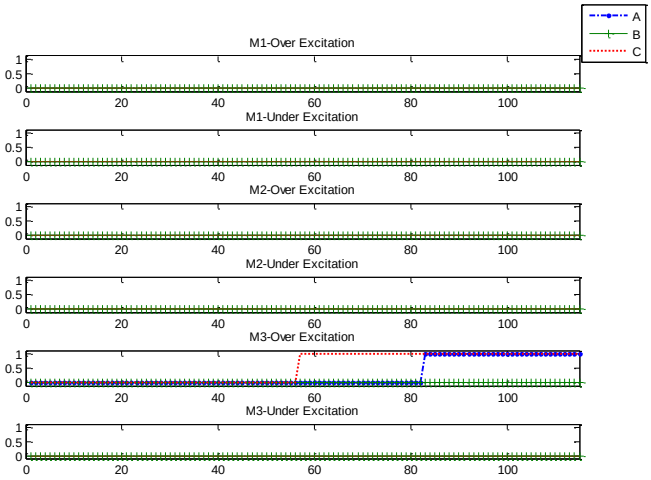

Fig.10. Alarm issued for detecting over excited and under excited condition detected at three measuring point.

On the other hand, variable generation units based on inverter technology are technically capable of providing steady-state and dynamic reactive power support to the grid. Therefore, FERC Order 661-A, demands the transmission operator to perform a system impact study, whether there is a need for a dynamic reactive capability, for wind farms, up to the 0.95 leading/lagging power factor range [17]. Meanwhile, some transmission service providers define certain reactive power requirements for wind power integration to their system. For example the Alberta Electric System Operator (AESO) defines the "Wind Power Facility Technical Requirements" (WPFTR) for integration of wind power facilities. Fig.11 shows the reactive power capability requirement defined by AESO [17], [32].

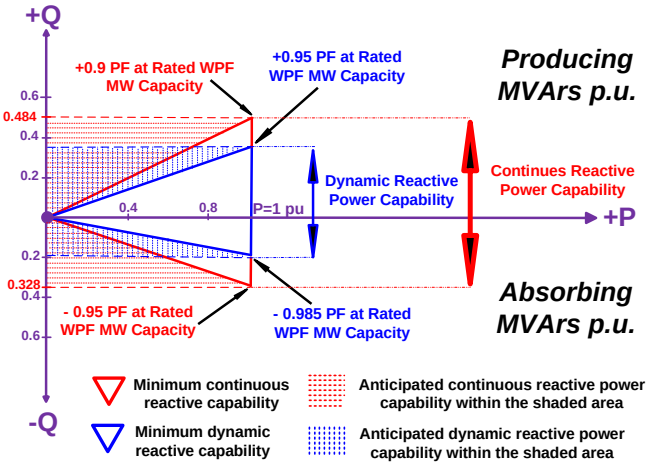

Fig 11. Reactive power capability requirement for AESO [17].

Although some utilities prefer static reactive power requirement, the AESO specifies both a dynamic range and a total range of reactive operation for wind farm integration. For example, AESO specifies a dynamic range of 0.95 lag to 0.985 lead and a total range of 0.95 lead, 0.90 lag, indicating a need for smooth and rapid operation between 0.95 lag to 0.985 lead, but allowing for some time delay for lagging power factors below 0.95.

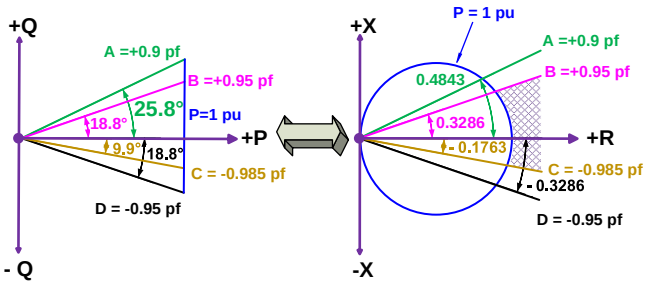

Fig.12 AESO reactive requirement curve mapped to R-X plane. The hatched area shows the mapped area correspond to dynamic range operation while P≤ 1pu.

To show the practical application of the impedance based monitoring system, the static and dynamic range of reactive power requirements curve will be mapped to *R-X* plane and then based on those defined criteria the monitoring system setting will be calculated. Fig. 12 shows mapping of the AESO defined area for reactive power requirement from *P-Q* plane into the *R-X* plane. It worth mentioning that, the hatched area in *R-X* plane in the Fig.12, shows the mapped area correspond to dynamic range operation while P≤ 1pu conditions in *P-Q* plane. In other words, for the conditions that the transferred power increases from the pre-defined nominal power of the line (P_0=1 pu) the mapped impedance will be settled down inside the circle.

For practical implementation of monitoring technique for AESO reactive requirement, the IEEE 8500 test feeder is modified as follows. The aggregated model of a 500 kW wind farm operating at pf=0.9 feeding to a large commercial load of 250 kW with pf=0.85 will be used in this section. In order to perform this, a 1 km, three phase line connected to bus m1026357 is added to IEEE 8500 node test feeder. The line parameters and wire size are the same as the main feeder data. Then the wind turbine and load are connected to end of this line. The nominal voltage of the line is 12.47 kV.

Three one-phase impedance measuring units (current and voltage transformers) installed at the bus m1026357 for each phase. In order to define the monitoring system direction, the polarity of the measuring units, designed in a way that the impedance measuring units monitor the point of interconnection (*POI*) from the wind farm perspective. Hence the measuring units monitor the line power flow.

As it was stated earlier the wind farm feeds the local load and the surplus power is sent to the grid. Therefore, the impedance measuring unit focuses on the changes of the total line power flow, not the changes of individual load or wind farm. Therefore, the resulting net power flow (wind power generation minus load) on each phase is monitored based on the AESO chart. The data used to in this section for wind turbine generation are 1-second wind power time series for 2900 consecutive seconds is shown in Fig.13 [29].

Fig. 14 shows the apparent impedance trends measured at *POI*, plotted on the mapped AESO reactive power requirement chart. While the impedance trend shows the reversed active and reactive power flow through the line for some time intervals, it can be seen that the impedance trend passes through the fixed PF lines. As the load value is fixed, this phenomena happens due to active and reactive power generation of wind turbine. Due to balanced loading, the impedance trends for the three phases are close to each other. Two different line nominal active power limits are defined for monitoring charts (P_n=50 kW (Blue circle) and P_n=70 kW (Brown circle) for each phase). It means that when the net active power flow of the line increases the limit of each phases, the measured impedance will pass through the corresponding circle. Note that for power flow beyond the power limit, the impedance settled down inside the circle and vice versa. Like section V.B different alarms can be defined for distribution system operator awareness, based on the defined regulation.

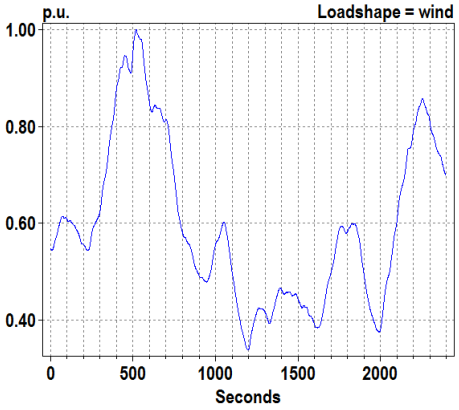

Fig.13 wind power profile example [29].

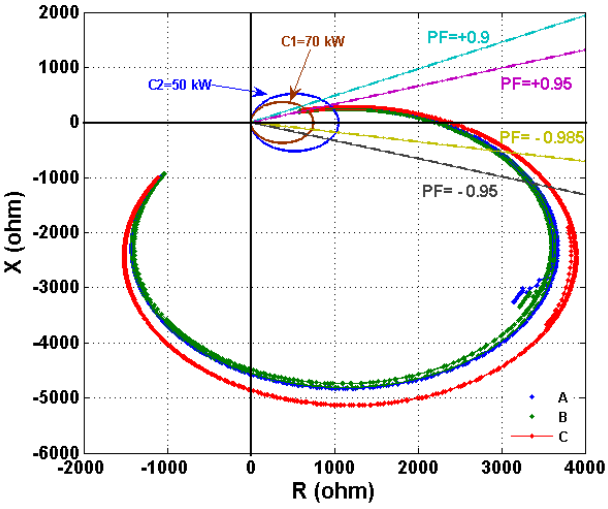

Fig 14.The output of three phase impedance measuring unit plot on the AESO reactive power requirement chart.

As it can be seen from Fig. 14, for a typical wind turbine power generation such as the Fig. 13, the reactive power requirement chart is violated more than once.

Therefore, for high penetration level of renewable energy integration, installation of real time monitoring devices such as the proposed method is recommended to ensure the reliable operation of distribution system.

VI. Conclusion

For a long time, the distribution system was designed based on the radial power flow assumptions. By integration of variable and intermittent RES to the distribution system, some assumptions (such as: radial power flow, little chance of over voltage happening and etc.) which were used as a basis for distribution system design are not true anymore.

This paper shows the necessity of online monitoring system for important feeders in distribution system. It was shown that the apparent impedance measured on the feeder has great capabilities for on line monitoring of distribution feeder.

The paper establishes the steady-state mathematical model for defining the monitoring zone in *R-X* plane as the main contribution. It was shown that the apparent impedance has a good potential for monitoring of feeder power factor, reverse and forward active and reactive power flow. In addition, it was shown that complex power curve can be transferred to R-X plane to monitor the reactive power requirement regulation issued by utilities for RES integration.

Authors are working on using this method for reactive power management in distribution system with high RES integration.

VII. References

[1] R. Billinton, R. N. Allan, and R. N. Allan, *Reliability evaluation of power systems* vol. 2: Plenum press New York, 1984.

[2] M. P. Tcheou, L. Lovisolo, M. V. Ribeiro, E. A. B. da Silva, M. A. M. Rodrigues, J. M. T. Romano, *et al.*, "The Compression of Electric Signal Waveforms for Smart Grids: State of the Art and Future Trends," *Smart Grid, IEEE Transactions on*, vol. 5, pp. 291-302, 2014.

[3] I. F. Visconti, D. A. Lima, J. M. C. de Sousa Costa, and N. Rabello de B.C.Sobrinho, "Measurement-Based Load Modeling Using Transfer Functions for Dynamic Simulations," *Power Systems, IEEE Transactions on*, vol. 29, pp. 111-120, 2014.

[4] F. Qiang, L. F. Montoya, A. Solanki, A. Nasiri, V. Bhavaraju, T. Abdallah, *et al.*, "Microgrid Generation Capacity Design With Renewables and Energy Storage Addressing Power Quality and Surety," *Smart Grid, IEEE Transactions on*, vol. 3, pp. 2019-2027, 2012.

[5] A. Bernieri, C. Liguori, and A. Losi, "Neural networks and pseudo-measurements for real-time monitoring of distribution systems," in *Instrumentation and Measurement Technology Conference, 1995. IMTC/95. Proceedings. Integrating Intelligent Instrumentation and Control., IEEE*, 1995, p. 112.

[6] M. E. Baran and A. W. Kelley, "A branch-current-based state estimation method for distribution systems," *IEEE transactions on power systems*, vol. 10, 1995.

[7] M. Baran, "Branch current based state estimation for distribution system monitoring," in *Power and Energy Society General Meeting, 2012 IEEE*, 2012, pp. 1-4.

[8] M. Ferdowsi, B. Zargar, F. Ponci, and A. Monti, "Design considerations for artificial neural network-based estimators in monitoring of distribution systems," in *Applied Measurements for Power Systems Proceedings (AMPS), 2014 IEEE International Workshop on*, 2014, pp. 1-6.

[9] M. Powalko, K. Rudion, P. Komarnicki, and J. Blumschein, "Observability of the distribution system," in *Electricity Distribution - Part 1, 2009. CIRED 2009. 20th International Conference and Exhibition on*, 2009, pp. 1-4.

[10] M. H. Bollen and F. Hassan, *Integration of distributed generation in the power system* vol. 80: John Wiley & Sons, 2011.

[11] H. Vahedi, P. A. Labb, x00E, and K. Al-Haddad, "Sensor-Less Five-Level Packed U-Cell (PUC5) Inverter Operating in Stand-Alone and Grid-Connected Modes," *IEEE Transactions on Industrial Informatics*, vol. 12, pp. 361-370, 2016.

[12] H. Vahedi and K. Al-Haddad, "Real-Time Implementation of a Seven-Level Packed U-Cell Inverter with a Low-Switching-Frequency Voltage Regulator," *IEEE Transactions on Power Electronics*, vol. 31, pp. 5967-5973, 2016.

[13] M. E. Baran, H. Hooshyar, S. Zhan, and A. Huang, "Accommodating High PV Penetration on Distribution Feeders," *Smart Grid, IEEE Transactions on*, vol. 3, pp. 1039-1046, 2012.

[14] W. H. Kersting, *Distribution system modeling and analysis*: CRC press, 2012.

[15] H. Mortazavi, H. Mehrjerdi, M. Saad, S. Lefebvre, D. Asber, and L. Lenoir, "A Monitoring Technique for Reversed Power Flow Detection With High PV Penetration Level," *Smart Grid, IEEE Transactions on*, vol. PP, pp. 1-1, 2015.

[16] H. Mortazavi, H. Mehrjerdi, M. Saad, S. Lefebvre, D. Asber, and L. Lenoir, "Application of distance relay in distribution system monitoring," presented at the IEEE PES General Meeting, Denver, USA. , 2015." In press".

[17] A. Ellis, R. Nelson, E. Von Engeln, R. Walling, J. MacDowell, L. Casey, *et al.*, "Reactive power performance requirements for wind and solar plants," in *Power and Energy Society General Meeting, 2012 IEEE*, 2012, pp. 1-8.

[18] P. Jahangiri and D. C. Aliprantis, "Distributed Volt/VAr Control by PV Inverters," *Power Systems, IEEE Transactions on*, vol. 28, pp. 3429-3439, 2013.

[19] T. A. Short, *Electric power distribution handbook*: CRC press, 2014.

[20] H. L. Willis, *Power distribution planning reference book*: CRC press, 2010.

[21] Y. Hase, *Handbook of Power System Engineering*, 2007.

[22] "IEEE Guide for the Application of Neutral Grounding in Electrical Utility Systems--Part IV: Distribution," *IEEE Std C62.92.4-2014 (Revision of IEEE Std C62.92.4-1991)*, pp. 1-44, 2015.

[23] C.-H. Kim, J.-Y. Heo, and R. K. Aggarwal, "An enhanced zone 3 algorithm of a distance relay using transient components and state diagram," *Power Delivery, IEEE Transactions on*, vol. 20, pp. 39-46, 2005.

[24] C. R. Mason, *The art and science of protective relaying*: Wiley, 1956.

[25] D. Tholomier, T. Yip, and G. Lloyd, "Protection of distributed generation (DG) interconnection," in *Power Systems Conference, 2009. PSC'09.*, 2009, pp. 1-15.

[26] "FERC Order No. 661-A, December 12, 2005.," ed.

[27] R. F. Arritt and R. C. Dugan, "The IEEE 8500-node test feeder," in *Transmission and Distribution Conference and Exposition, 2010 IEEE PES*, 2010, pp. 1-6.

[28] M. J. Reno and K. Coogan, "Grid Integrated Distributed PV (GridPV) Version 2," *Sandia National Labs SAND2014-20141*, 2014.

[29] R. C. Dugan, "Reference Guide: The Open Distribution System Simulator (OpenDSS)," *Electric Power Research Institute, Inc*, 2012.

[30] M. U. s. Guide, "The mathworks," *Inc., Natick, MA*, vol. 5, 1998.

[31] A. Hoke, R. Butler, J. Hambrick, and B. Kroposki, "Steady-state analysis of maximum photovoltaic penetration levels on typical distribution feeders," *Sustainable Energy, IEEE Transactions on*, vol. 4, pp. 350-357, 2013.

[32] S. El Itani and G. Joós, *Advanced wind generator controls: meeting the evolving grid interconnection requirements*: INTECH Open Access Publisher, 2012.